*Journal of Ceramic Processing Research. Vol. 25, No. 3, pp. 345~354 (2024)*
*(Received 6 January 2024, Received in revised form 7 February 2024, Accepted 15 February 2024)*
*https://doi.org/10.36410/jcpr.2024.25.3.345*

J O U R N A L O F
**Ceramic Processing Research**

# Application of ceramic waste aggregates in fly ash, metakaolin, and silica fume based geopolymer concrete

**C. Chinnaraj[a,*], K. Subramanian[b] and P. Muthupriya[c]**
[a]*Assistant Professor, Department of Civil Engineering, RVS Technical Campus- Coimbatore*
[b]*Professor, Department of Civil Engineering, PSR Engineering College, Virudhunagar*
[c]*Professor and head, Department of Civil Engineering, Dr.N.G.P. Institute of Technology, Coimbatore*

**The study introduces an innovative approach to utilise ceramic waste aggregates (CWA) in the production of environmentally friendly geopolymer concrete (GPC), as a substitute for conventional coarse aggregates (CCA). This novel method involves the incorporation of class F fly ash (FFA), metakaolin (MK), silica fume (SF) and alkali activators to create the geopolymer concrete. The main purpose of this study is to investigate the mechanical, mineralogical and microstructural properties of FFA, MK and SF in GPC. The results of the investigation reveal a positive synergistic effect among FFA, MK, and SF, leading to enhanced mechanical and microstructural performance of CWA-based GPCs compared to OPC concrete. Among the various mix designs, the F30M50S20 combination exhibits the highest compressive strength (48.5 MPa), flexural strength (6.85 MPa), and split tensile strength (4.14 MPa). Microstructural and mineralogical analyses conducted using SEM, XRD, and TGA techniques illustrate the densification of the matrix and the development of C-S-H gel. Moreover, the formation of mullite mineral is also observed, which could be attributed to the improved performance of GPCs. This study demonstrates the feasibility and advantages of incorporating ceramic waste aggregates into geopolymer concrete.**

**Keywords: Ceramic waste aggregates, Geopolymer concrete, Mechanical properties, Microstructural analysis, Mineralogical analysis, Sustainable construction.**

## Introduction

Concrete is a fundamental material in the construction industry and plays an important role in building infrastructure. Its strength, durability, and versatility make it a preferred choice for various applications. However, concrete production significantly contributes to environmental hazards. The process of making cement, a key component of concrete, involves high-temperature heating of raw materials, releasing substantial amounts of carbon dioxide into the atmosphere. Furthermore, mining of aggregates and transportation of materials contribute to air pollution and habitat destruction. The mining of raw materials can disrupt ecosystems which leads to landscape deprivation. Thus, while concrete is essential for modern construction, addressing its environmental impact is crucial to ensure sustainable development and minimise harm to the environment [1].

Geopolymer concrete is a cementitious material that utilises geopolymers as the primary binder instead of Portland cement. It is developed by blending materials with a high content of silica and alumina, with an alkaline activator solution containing alkali metal hydroxides and alkali metal silicates [2]. The alkaline activator initiates a complex chemical reaction known as geopolymerization, where the source materials undergo polycondensation, resulting in the formation of a highly cross-linked three-dimensional polymeric structure. This geopolymeric network provides the binding and solidification of the concrete mixture [3].

Geopolymer concrete exhibits several notable technical advantages over conventional concrete. Firstly, it offers reduced carbon emissions since it utilises industrial by-products and waste materials as precursors, mitigating the need for energy-intensive cement production [4]. Additionally, geopolymer concrete displays enhanced durability characteristics, including improved resistance to chemical attacks, corrosion, and fire [5]. It possesses a lower permeability compared to ordinary Portland cement concrete, enhancing its resistance to moisture ingress and the detrimental effects of freeze-thaw cycles [6]. Moreover, geopolymer concrete demonstrates superior mechanical properties, both in the early and long-term periods. Its strength development is influenced by the chemical composition of the source materials, activator concentration, curing conditions and geopolymerization kinetics. The exceptional strength performance makes geopolymer concrete suitable for various structural applications requiring high load-bearing capacity [7]. Moreover, geopolymer concrete exhibits a reduced risk of

*Corresponding author:
Tel : +91 97906 50333
E-mail: erchinnaraj.civil@gmail.com

alkali-silica reaction. The use of geopolymers eliminates or significantly mitigates this issue, contributing to the long-term durability and service life of structures [8, 9].

In recent periods, the interest in sustainable supplementary cementitious materials to foster sustainable development has risen tremendously. Ceramics are widely used globally, and they generate a significant amount of waste, with approximately 15-30% being disposed of or found on demolition sites. The accumulation of Ceramic Waste (CW) poses severe environmental problems and consumes valuable landfill space [10].

To address these challenges, efforts have been made to incorporate CW into concrete as a partial alternative for cement and aggregates. A study on concrete with ceramic waste coarse aggregate found that ceramic waste could be effectively developed into valuable aggregates. The resulting concrete had properties comparable to conventional concrete-making aggregates. Although the concrete with CW aggregate exhibited slightly lower compressive, splitting tensile, and flexural strengths (by 3.8%, 18.2%, and 6% respectively), it showed a lesser tensile-to-compressive strength ratio [11].

Medina, Sánchez de Rojas and Frías [12] reused sanitary ceramic waste as recycled coarse aggregate in concretes, partially replacing natural coarse aggregates (15%, 20%, and 25%). The results showed that the recycled concrete exhibited better mechanical properties than conventional concrete. Notably, the sanitary ceramic waste aggregate did not negatively impact the hydration process. Furthermore, the microstructure was denser compared to the natural aggregate and paste, indicating the potential for sustainable concrete production.

Elçi [13] explored the feasibility of utilising crushed floor and wall tile waste as aggregates, aiming to reduce manufacturing costs and environmental impact. Concrete properties using tile aggregates were compared with natural aggregates. Concrete made with crushed aggregates exhibited similar mechanical properties to limestone concrete.

Kannan, Aboubakr, El-Dieb and Reda Taha [14] explored the use of CWP as a partial replacement for Portland cement in high-performance concrete. Results revealed that mixtures incorporating 10-40% CWP exhibit enhanced strength and durability. Microstructural examination demonstrated that CWP did not significantly affect cement hydration. The performance improvement was attributed to the low water-to-cement ratio, allowing CWP to create a dense particle packing.

El-Dieb, Taha, Kanaan and Aly [15] conducted a study investigating the incorporation of ceramic waste powder (CWP) in conventional and self-compacting concrete production. The research aimed to promote the recycling of landfill material, reduce the environmental impact of cement production, and conserve natural resources. CWP, mainly comprising silicon dioxide and aluminium oxide, was used as a partial replacement for cement in concrete mixtures at different levels. The findings revealed the successful utilization of CWP as a partial cement replacement in both concrete types, with optimal replacement levels depending on the concrete's strength grade. For conventional concrete, replacements between 10% to 30% were suitable, while for self-compacting concrete, 28% or 57% replacements were found to be acceptable.

Suzuki, Seddik Meddah and Sato [16] explored the effectiveness of utilising "recycled waste porous ceramic coarse aggregates" (PCCA) for curing high-performance concrete (HPC) internally to reduce autogenous shrinkage and early-age cracking. Different silica fume HPC mixtures with varying proportions of PCCA replacement were examined. Results demonstrated that incorporating 40% PCCA led to non-shrinking HPC with increased compressive strength. Internal water curing with PCCA improved cement hydration and reduced autogenous shrinkage by up to 105%. The reduction in autogenous shrinkage resulted in a decrease in internal capillary tensile stress and enhanced compressive strength by 10% to 20%.

Subaşı, Öztürk and Emiroğlu [17] investigated the application of granulated powdered waste ceramic (WCP) in self-consolidating concrete (SCC). SCC benefits from fine fillers (<0.125 mm) to enhance fresh state properties, strength and durability. WCP replaced cement at 5%, 10%, 15%, and 20% by weight in SCC mixtures. While WCP positively affected mix viscosity, there was a slight decrease in strength compared to pure cement mixes. It was concluded that finely ground WCP up to 15% can be considered as a filler material for SCC production when strength and flowability parameters are jointly evaluated.

Huseien, Sam, Shah, Mirza and Tahir [18] evaluated alkali-activated mortars (AAMs) containing waste ceramic powder (WCP) and fly ash (FA) as a replacement for ground blast furnace slag. FA enhanced AAMs' durability and resistance to hostile environments such as acid, sulphate, and elevated temperatures. The AAMs with 40% FA achieved high compressive strength (45.9 MPa).

In a study by López, Llamas, Juan, Morán and Guerra [19], an exploration was conducted into the physical and mechanical attributes of laboratory-created concrete that integrated different ratios of white ceramic powder as fine aggregate. This ceramic powder was sourced from a combination of demolition site debris and waste originating from the ceramic industry. Notably, the concrete exhibited mechanical properties comparable to traditional sand-based concrete. Impressively, the compressive strength was either maintained or even improved, negating any reduction. Furthermore, the introduction of white ceramic powder did not impact the traction resistance of the resulting concrete.

Torkittikul and Chaipanich [20] explored the application of ceramic waste as fine aggregate in concretes. Crushed ceramic waste fragments were utilised as fine aggregates.

Workability decreased with a rise in ceramic waste content in both types of concrete, except for fly ash concrete with 100% ceramic waste, which maintained sufficient workability. Compressive strength increased with ceramic waste content up to 50% in Portland cement concrete but dropped beyond 50% due to reduced workability. In contrast, fly ash concrete showed continual strength increase with higher ceramic waste content.

Kim and Kimd [21] investigated the mechanical properties of lightweight geopolymers containing integrated gasification combined cycle slag and Si sludge under various curing conditions and immersion periods. Autoclaved specimens exhibited abrupt breakdown characteristics, while oven-cured specimens displayed dentable characteristics. After 7 days of immersion, dentable characteristics disappeared, but autoclaved specimens maintained stability, indicating complete geopolymerization; an additional drying process increased compressive strength significantly, likely by promoting geopolymerization. Optimal specimens were obtained from larger specimens by controlling the W/S ratio and particle size, achieving low density (0.74 g/cm$^3$) and high compressive strength (8.1 MPa), highlighting the potential for controlled process factors in lightweight geopolymer production [22]. Si sludge incorporation led to large pores and uneven distributions, impacting mechanical properties negatively. Optimal curing at 123 °C in an autoclave resulted in the highest compressive strength after immersion, ensuring stable mechanical properties in wet environments [23].

The properties of alumino-silicate geopolymer using mine tailings, coal fly ash, granulated blast furnace slag, and alkali activator were investigated. Compressive strength peaked at 142.2 MPa, decreased with increasing mine tailings addition and curing days. Alumino-silicate geopolymer with mine tailings showed higher compressive strength than Portland cement mortar, with heavy metal ions leaching below toxic thresholds, indicating effective stabilization [24]. The potential of recycling Malaysia's Electric Arc Furnace (EAF) steel slag waste for geopolymer ceramic production, assessing formulations with and without China clay in alkaline conditions was explored. Variations in curing temperature were investigated, with XRD, XRF, and FTIR characterizing the chemical and mineralogical properties, while physical properties like water absorption and compressive strength were evaluated, showing promising results aligned with observed phase analysis and functional groups [25].

Tian, Sun, Gu and Lv [26] examined the impact of alkaline activator characteristics on compressive strength and microstructure of fly ash-based geopolymer pastes. Higher $Na_2O$ content and modulus (Ms) of the activator solution increased compressive strength, while higher water-to-binder (W/B) ratios decreased it. Optimal compressive strength (26.5-39.6 MPa) was achieved with Ms at 1.5 and alkaline activator content at 8.0-12.0% of $Na_2O$ to fly ash proportion. OH- concentration, influenced by $Na_2O$ content, Ms, and water content, was crucial for achieving appropriate geopolymer paste strength, with increased alkaline content promoting the formation of N-A-S-H gel.

Rho [27] synthesized and characterized lightweight foamed geopolymers based on metakaolin, analyzing the effect of replacing Al powder with Si sludge as a foaming agent. While specimens foamed with Al powder had lower density, they exhibited higher compressive strength due to a more uniform pore distribution. Lightweight foamed geopolymers with densities ranging from 0.36 to 1.05 g/cm$^3$ and compressive strengths from 0.7 to 4.7 MPa were achieved by controlling process conditions, demonstrating the potential of Si sludge as a replacement for Al powder. The resulting geopolymers offer versatile applications meeting the required physical properties for various fields.

The present study focuses on utilising waste tiles as a complete substitute for conventional coarse aggregates in geopolymer concrete. While some research has been conducted on waste ceramics-based geopolymer concrete, there is a lack of specific investigations on geopolymer concrete using floor and wall tiles as coarse aggregate and fly ash, metakaolin, and silica fume as precursors. The primary aim is to explore the feasibility and potential benefits of incorporating waste tiles as a sustainable substitute material in geopolymer concrete.

## Materials and Properties

### Aggregates

The granite rock was crushed and used as Conventional Coarse Aggregate (CCA) in this research. For fine aggregate, River Sand (RS) was used. These materials were purchased from a leading building materials supplier in Coimbatore. The Ceramic Waste Aggregate (CWA) was prepared by grounding the waste floor and wall tiles collected from various construction sites located in Coimbatore. The gradational characteristics of the aggregates along with the Indian Standards (IS) limits for aggregates are presented in Fig. 1. The RS falls under zone II while the CCA and CWA have a majority of the particle sizes between 10 mm-20 mm. Further, the physical characteristics of the aggregates are shown in Table 1. The CCA exhibited a higher specific gravity of 2.7, indicating greater density compared to the CWA with a specific gravity of 2.47. Moreover, the CCA also showed a slightly higher fineness modulus of 7.12, implying coarser particles compared to the CWA's value of 6.9. On the other hand, the CWA demonstrated marginally better water absorption (1.94% compared to 2.04% for CCA). However, the CCA exhibited superior impact resistance (13.38% compared to 17.91% for CWA) crushing resistance (14.57% compared to 16.27% for CWA), and abrasion resistance (12.88% compared

**Table 1.** Physical characteristics of the aggregates.

| Properties | RS | CCA | CWA |
|---|---|---|---|
| Specific gravity | 2.65 | 2.7 | 2.47 |
| Fineness modulus | 2.94 | 7.12 | 6.9 |
| Water absorption (%) | 1.77 | 2.04 | 1.94 |
| Impact value (%) | - | 13.38 | 17.91 |
| Crushing value (%) | - | 14.57 | 16.27 |
| Abrasion value (%) | - | 12.88 | 14.43 |

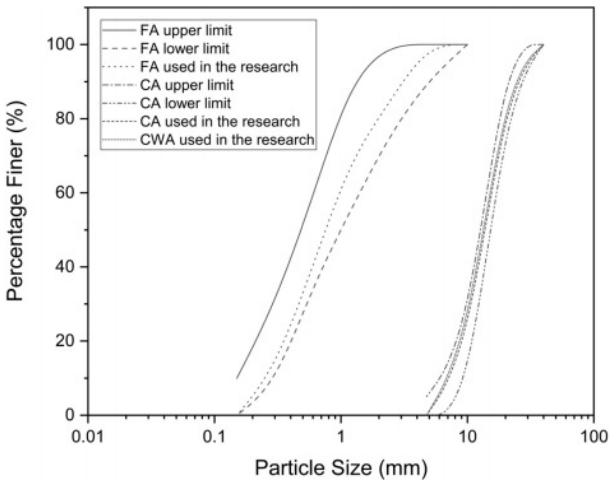


**Fig. 1.** Particle size distribution of aggregates.

to 14.43% for CWA). These properties are in line with the IS specifications.

## Precursors

The present study utilised Ordinary Portland Cement (OPC) 53 grade adhering to the Indian standard [28] for making conventional concrete. The OPC had a specific gravity of 3.15 and an initial setting time of 30 minutes. Flyash belonging to the Class F (FAF) category was sourced from a thermal power plant located in Salem district, Tamil Nadu, India. Metakaolin (MK) and Silica Fume (SF) were purchased from the local market. The Specific gravities of FAF, MK, and SF were 2.23, 2.54 and 2.27 respectively. The chemical compositions of FAF, MK, and SF are shown in Table 2.

**Table 2.** Chemical composition of precursors.

| Elements (% by weight) | OPC | FAF | MK | SF |
|---|---|---|---|---|
| $SiO_2$ | 25.3 | 57.55 | 53.05 | 94.26 |
| $Al_2O_3$ | 3.31 | 29.85 | 44.18 | 0.14 |
| CaO | 66.58 | 3.07 | 0.16 | 0.28 |
| MgO | 1.29 | 0.46 | 0.51 | 0.16 |
| $Fe_2O_3$ | 1.96 | 3.36 | 0.72 | 0.84 |
| $SO_3$ | 0.22 | 0.15 | 0 | 0.32 |
| $Na_2O$ | 0 | 0.13 | 0.11 | 0 |
| $K_2O$ | 0.81 | 1.52 | 0.04 | 0.65 |
| $TiO_2$ | 0.34 | 3.14 | 0.57 | 0.61 |
| SrO | 0 | 0.31 | 0 | 0.56 |
| $P_2O_5$ | 0.2 | 0.46 | 0.62 | 1.24 |
| MnO | 0 | 0 | 0.03 | 0.94 |

## Alkali activators

Alkaline activator solutions used in this study consisted of NaOH and $Na_2SiO_3$. A 15 M NaOH solution and a solution of $Na_2SiO_3$ were utilised. The ratio of $Na_2SiO_3$ to NaOH solutions was maintained at 2.0, which was determined based on previous research [29]. Before its use in the preparation of Geopolymer Concrete, the activator solution was kept at laboratory temperature (27°C) for 24 hours.

# Concrete Mix Ratios and Mixing Technique

The present study considered 8 different mix ratios consisting of two mixes made with OPC and six geopolymer mixes. The OPC mix with CCA was considered a benchmark mix and designated as OPC-CCA. The mix OPC-CWA was the modification of the OPC-CCA mix in which the coarse aggregate was replaced with CWA. Out of six geopolymer mixes, 3 mixes were developed by incorporating FAF and MK

**Table 3.** Mix ratios of concrete examined in this study.

| Mix designation | Cementitious compounds ($kg/m^3$) | | | | Sand ($kg/m^3$) | CCA ($kg/m^3$) | CWA ($kg/m^3$) | Water ($kg/m^3$) | NaoH | $Na_2Sio_3$ |
|---|---|---|---|---|---|---|---|---|---|---|
| | OPC | FA | MK | SF | | | | | | |
| OPC-CCA | 405 | | | | 681 | 1151 | | 154 | | |
| OPC-CWA | 405 | | | | 681 | | 1052 | 154 | | |
| F70M30 | | 283.5 | 121.5 | | 681 | | 1052 | | 51.33 | 102.67 |
| F60M40 | | 243 | 162 | | 681 | | 1052 | | 51.33 | 102.67 |
| F50M50 | | 202.5 | 202.5 | | 681 | | 1052 | | 51.33 | 102.67 |
| F40M50S10 | | 162 | 202.5 | 40.5 | 681 | | 1052 | | 51.33 | 102.67 |
| F35M50S15 | | 141.8 | 202.5 | 60.8 | 681 | | 1052 | | 51.33 | 102.67 |
| F30M50S20 | | 121.5 | 202.5 | 81 | 681 | | 1052 | | 51.33 | 102.67 |

while the other 3 mixes were produced by incorporating FAF, MK, and SF. For instance F70M30 mix contained 70% of FAF and 30% of MK and the F35M50S15 mix had 35% of FAF, 50% of MK and 15% of SF. The details of the mixes are presented in Table 3.

The concrete mixing process involved dry blending FFA, MK, SF, and RS in a pan. Then, CWA was supplied to the mixer, and mixing continued. The alkaline solution was gradually introduced, and wet mixing took place. The mixing time was maintained at two to three minutes at each stage. The fresh concrete was poured into three sets of moulds of 150 mm side cubes, 100 mm × 200 mm cylinder and 100 mm × 100 mm × 500 mm. These specimens were further placed at room temperature for a day and then subjected to submergence in water until tested.

## Results and Discussion

### Slump of fresh concrete

Figure 2 presents the slump values (in mm) for different concrete mix designs using various aggregate combinations. When comparing the two types of aggregates, it was observed that the OPC-CWA mix exhibited a slightly higher slump value (122 mm) compared to the OPC-CCA mix (114 mm). This suggested that the CWA contributed to a slightly more workable concrete compared to the CCA. As the water absorption of CWA is relatively lower than the CCA, an increase in workability was achieved. Geopolymer concrete exhibited decreased workability compared to OPC-based concrete due to the higher viscosity of its paste during the geopolymerization process. The chemical reaction of aluminosilicate materials with alkaline activators led to the formation of a more viscous mixture, making it challenging for particles to flow and move easily. Moreover, Replacing FFA with MK in concrete mixtures typically led to a reduction in the slump value. This was primarily due to the difference in particle size, shape, and pozzolanic activity between the two materials. FFA had fine, spherical particles that enhanced workability and flow, resulting in a higher slump value. In contrast, MK had smaller and irregularly shaped particles, which may hinder lubrication and reduce workability, leading to a lower slump value. Additionally, MK generally had a higher water demand and adjusting the water content to maintain a consistent water-cement ratio further affected the slump value. Furthermore, Silica fume particles had a high surface area, which resulted in increased water demand. The fine particles tended to absorb water, causing the mixture to become drier. As a result, the overall workability of the concrete decreased. Silica fume particles had a spherical shape and were extremely small in size. When these particles were dispersed in the cementitious matrix, they tended to fill the gaps between the larger particles, such as cement and aggregate particles. This filling effect

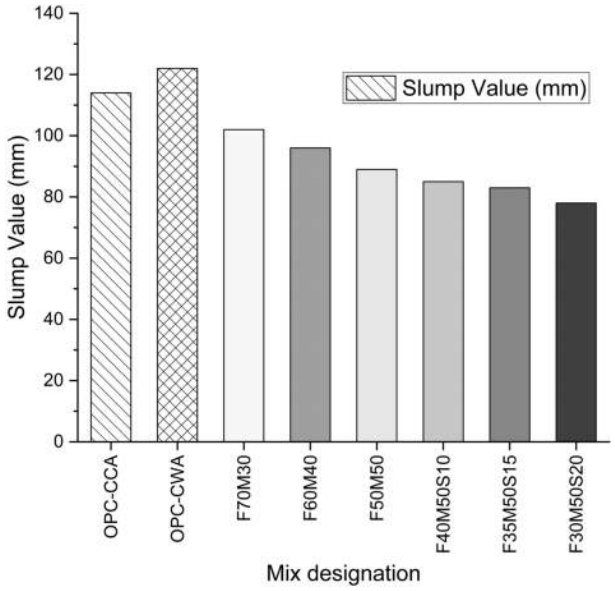


**Fig. 2.** Flow characteristics of concrete mixes.

increased the viscosity, making it more difficult to move and shape. Consequently, the workability decreased. The inclusion of SF affected the packing of particles in the concrete mixture. As SF had a small particle size, it could fill in the voids present among the larger particles, resulting in a denser packing. This densification reduced the lubrication between the particles and made it more difficult for them to slide past one another, thereby reducing the workability.

### Strength characteristics

The strength of concrete mixes under compression, tension and flexure at different curing periods are presented in Table 4. At 7 days, the mix OPC-CCA exhibited the highest compressive strength of 34.4 MPa, followed by OPC-CWA with 31.3 MPa. Among the geopolymer mixes, F30M50S20 achieved the highest compressive strength of 32.9 MPa at 7 days. Over 28 days, the compressive strengths improved across all mixes, with OPC-CCA leading at 46.2 MPa, OPC-CWA at 42.7 MPa, and F30M50S20 at 48.5 MPa. The OPC-CCA mix had the highest tensile strength among all mixes, reaching 2.45 MPa at 7 days and 3.59 MPa at 28 days. The geopolymer mixes generally exhibited lower tensile strengths. At 7 days, F70M30 had the lowest tensile strength (1.14 MPa), while F30M50S20 showed the highest (2.4 MPa). These values increased for all mixes at 28 days, with F30M50S20 having the highest tensile strength of 4.14 MPa. OPC-CCA demonstrated the highest flexural strength at both 7 days (4.45 MPa) and 28 days (6.02 MPa). Among the geopolymer mixes, F30M50S20 displayed the highest flexural strength of 6.85 MPa at 28 days. The flexural strengths generally increased with curing time for all mixes.

The OPC-CCA mix attained the maximum strength

**Table 4.** Strength characteristics of various mix ratios.

| Mix designation | Compressive Strength (MPa) | | Tensile Strength (MPa) | | Flexural Strength (MPa) | |
|---|---|---|---|---|---|---|
| | 7 days | 28 days | 7 days | 28 days | 7 days | 28 days |
| OPC-CCA | 34.4 | 46.2 | 2.45 | 3.59 | 4.45 | 6.02 |
| OPC-CWA | 31.3 | 42.7 | 1.97 | 3.14 | 3.62 | 5.38 |
| F70M30 | 18.6 | 31.3 | 1.14 | 2.06 | 2.16 | 3.86 |
| F60M40 | 20.6 | 37.8 | 1.35 | 2.88 | 2.44 | 4.81 |
| F50M50 | 24.8 | 40.1 | 1.71 | 3.19 | 3.05 | 5.32 |
| F40M50S10 | 26.1 | 42.3 | 1.84 | 3.39 | 3.24 | 5.75 |
| F35M50S15 | 27.4 | 44.6 | 1.98 | 3.67 | 3.52 | 6.13 |
| F30M50S20 | 32.9 | 48.5 | 2.4 | 4.14 | 4.47 | 6.85 |

in all loading conditions and at various curing periods compared to the OPC-CWA mix due to several factors. CCA showed superior performance in mechanical tests such as impact, crushing, and abrasion values implying better durability and strength. Moreover, the inherent strength of natural rock-based CCA contributes to its higher strength potential of OPC-CCA mix, along with potential advantages in bonding and load transfer.

Comparing the benchmark OPC-CCA mix to the geopolymer mixes, it is evident that the geopolymer mixes generally had lower early strengths (at 7 days) but exhibited competitive strengths at 28 days. This could be attributed to the different settings and curing mechanisms of geopolymer concrete compared to traditional OPC-based concrete. For example, the compressive strengths of mixtures F70M30, F60M40, and F50M50 were measured at 31.3 MPa, 37.8 MPa, and 40.1 MPa respectively. The increase in strength with a decrease in FFA content and an increase in MK content in geopolymer concrete could be attributed to the specific properties and contributions of these materials to the geopolymerization process.

The enhancement in compressive strength of FFA-MK geopolymers was attributed to the increasing content of MK, leading to improved geopolymerization and a denser microstructure. This effect rose from the remarkable reactivity of MK particles, which fostered extensive geopolymerization. Consequently, geopolymers with higher MK content exhibited notably greater compressive strength compared to those with lower MK content, as indicated by previous studies [30, 31]. Similar tendencies were observed in relation to other mechanical properties.

Elevating the MK content was also found to elevate the splitting tensile strength, increasing it from 2.06 MPa to 3.19 MPa for mixes F70M30 and F50M50, respectively. Additionally, the flexural strength ranged from 3.86 MPa to 5.32 MPa for the same mixes, F70M30 and F50M50. These outcomes unequivocally validated the notion that the utilisation of MK positively influenced the strength characteristics of geopolymer concretes. This improvement could be attributed to MK's fine particle size, which enhanced the microstructure of the interfacial transition zone (ITZ). Consequently, this refinement enhanced the bonding between the pastes and recycled aggregates [30, 31].

Moreover, the correlations between the compressive strength of concrete ($f_c$) and both its tensile strength ($f_t$) and flexural strength ($f_f$) have been established and visually represented in Fig. 3. The correlation between the compressive strength of concrete and its tensile strength yielded an $R^2$ value of 0.9735, while the relationship between compressive strength and flexural strength produced an $R^2$ value of 0.9824. These empirical equations could serve as valuable tools for predicting the tensile and flexural strengths of concrete based on its known compressive strength.

The UPV values for various concrete mix designs are presented in Fig. 4. These UPV measurements could serve as indicators of the internal quality and integrity of the concrete specimens. The UPV values exhibited variations across different mix compositions. The mix OPC-CCA recorded the highest UPV value, registering at 3930 m/s. This result suggested that the combination of OPC and CCA could lead to a concrete mixture with

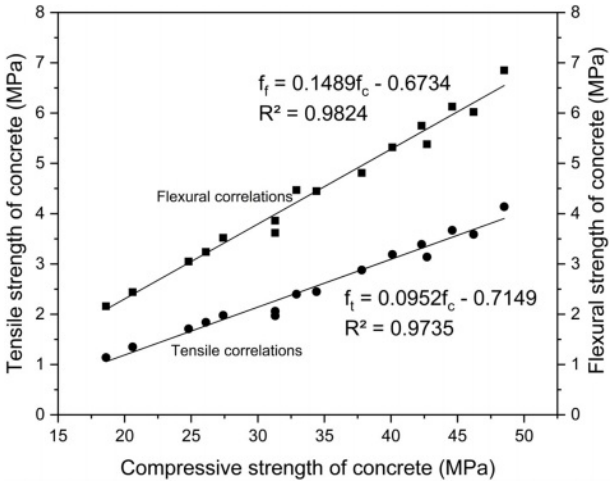


**Fig. 3.** Correlation among strength characteristics.

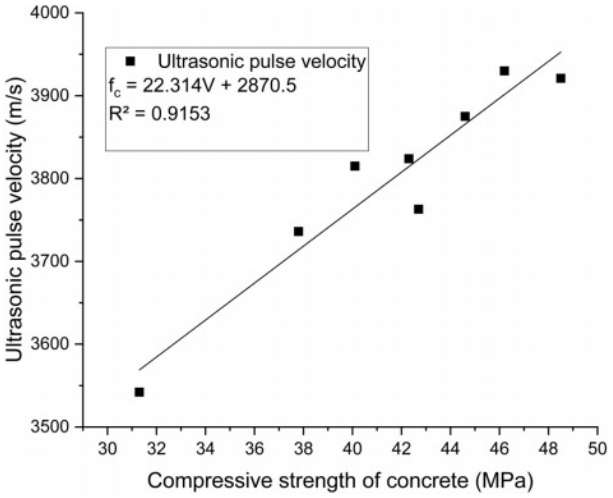


**Fig. 4.** Correlation between UPV and Compressive strength.

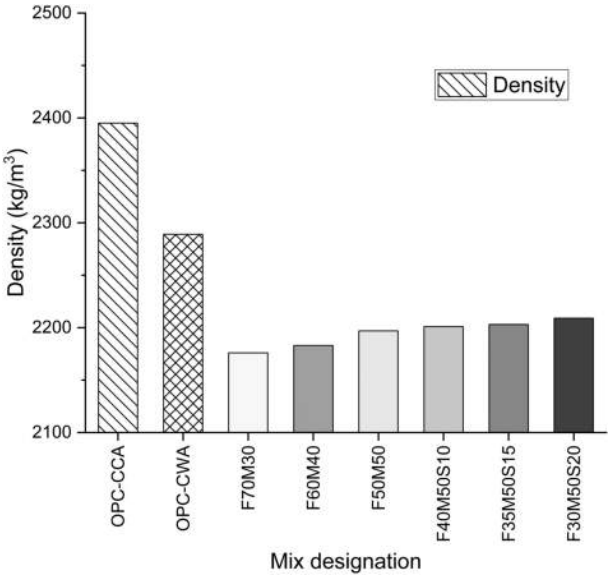


**Fig. 5.** Density of various mixes.

superior internal homogeneity and structural integrity. In contrast, the mix OPC-CWA yielded a slightly lower UPV value of 3763 m/s. The presence of waste aggregates could potentially introduce variability in material properties, which might have contributed to the observed difference in UPV compared to the OPC-CCA mix.

Transitioning to geopolymers, a notable trend is observed where the UPV values align with the compressive strength trends. The mix labelled as F70M30, with a lower MK content, exhibited a UPV value of 3542 m/s. This value was surpassed by F60M40 and F50M50, with UPV values of 3736 and 3815 m/s respectively. This increase in UPV with increasing MK content reflects the intricate relationship between geopolymerization and internal microstructural characteristics.

Intriguingly, the incorporation of SF, along with MK influenced the UPV results. Mix F40M50S10, containing 10% SF, displayed a UPV value of 3824 m/s. Similarly, mixes F35M50S15 and F30M50S20, with 15% and 20% SF content respectively, showed UPV values of 3875 and 3921 m/s. This suggests that the combined effect of MK and SF has a positive impact on the internal soundness and quality of the concrete, potentially influencing factors such as pore structure and interfacial bonding.

Further, a correlation between the 28-day compressive strength and ultrasonic pulse velocity (UPV, denoted as V) has been established and visually depicted in Figure 5. The equation governing this relationship yielded an $R^2$ value of 0.9153, indicative of a robust and substantial connection. This equation presented promising utility for non-destructive applications, enabling the estimation of compressive strength through UPV measurements.

## Density characteristics

The density of various concrete mix designs is presented in Fig. 5. The density of concrete mixtures varies across different compositions. The mix OPC-CCA exhibited a density of 2395 kg/m³, while the mix containing OPC-CWA displayed a slightly lower density of 2289 kg/m³. This difference in density was attributed to the varying characteristics of the aggregate materials, wherein the specific gravities of CCA and CWA contribute to the overall density of the respective mixes.

Transitioning to geopolymers, a consistent trend emerged where the density values increased as the MK content increased. Mix F70M30 demonstrated the lowest density at 2176 kg/m³. Similarly, mixes F60M40 and F50M50 exhibited densities of 2183 kg/m³ and 2197 kg/m³ respectively. Furthermore, incorporating SF along with MK, influenced the density of the concrete mixtures. Mix F40M50S10 displayed a density of 2201 kg/m³. Similarly, mixes F35M50S15 and F30M50S20 exhibited densities of 2203 kg/m³ and 2209 kg/m³. This suggested that the addition of SF along with MK had a discernible effect on the density of the final concrete mixtures.

To interpret these density variations in the broader context, it's crucial to consider the specific gravity values of the materials used. MK possesses a specific gravity of 2.54, while FFA and SF exhibit specific gravities of 2.23 and 2.27 respectively. These values highlight the relative density of these materials and contribute to the overall density observed in the concrete mixtures.

## Mineralogical characteristics

### XRD Analysis

The XRD patterns displayed in Fig. 6 offer insights into the mineralogical composition of diverse geopolymer mixes. The XRD patterns of various geopolymer mixes showed the presence of three main crystalline phases: quartz, calcium silicate hydrate (CSH) and mullite. The intensity of the peaks in the XRD patterns varied according to the composition of the geopolymer mix. The mixes with SF showed high-intensity peaks compared

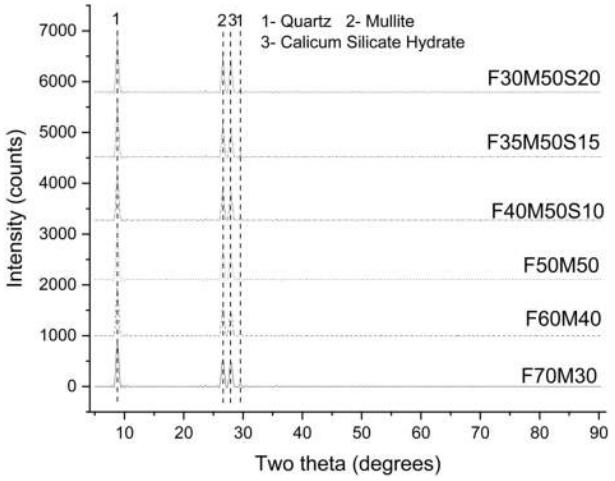


**Fig. 6.** XRD patterns of different mixes.

to the other mixes, indicating that the SF mixes had a higher proportion of geopolymeric compounds. This is because SF is a more reactive aluminosilicate material than FFA or MK. The higher proportion of geopolymeric compounds in the SF mixes resulted in improved mechanical properties and durability [32, 33]. This validated the strength characteristics of the study.

**TGA Analysis**

Figure 7 presents the loss of mass of different mixes as a function of temperature. The extent of mass loss, ranging from 2.5% to 6.5% at a temperature of 1200 °C, exhibited variability based on the composition of the mixture. Notably, geopolymer concretes containing SF displayed higher mass loss, attributed to the likely formation of an increased amount of geopolymer gel. The TGA profiles manifested distinct phases, which could be categorized into four zones. The initial weight reduction, occurring below 100 °C (zone I), was credited to the expulsion of hygroscopic water. The subsequent phase, spanning 100 to 300 °C (zone II), corresponded to the release of structural water embedded within the geopolymer gel [34, 35]. In zone I, the mass loss was approximately 1%, while in zone II, it ranged from 1.0% to 3.0%. The interval between 300 °C and roughly 800 °C (zone III) demonstrated a continuous decrease in weight. This phenomenon was linked to the removal of

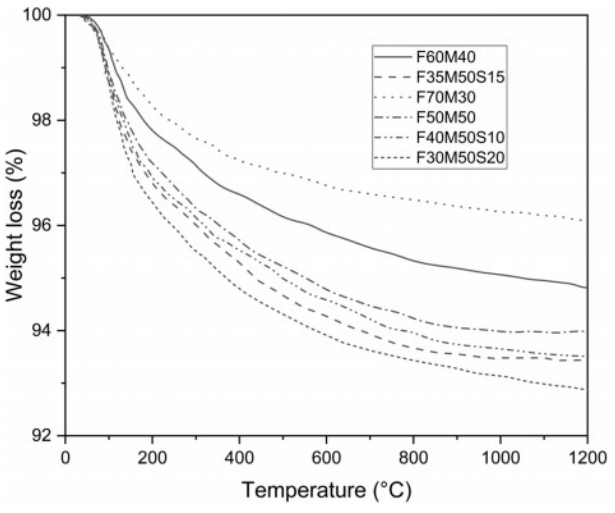


**Fig. 7.** TGA of various geopolymer mixes.

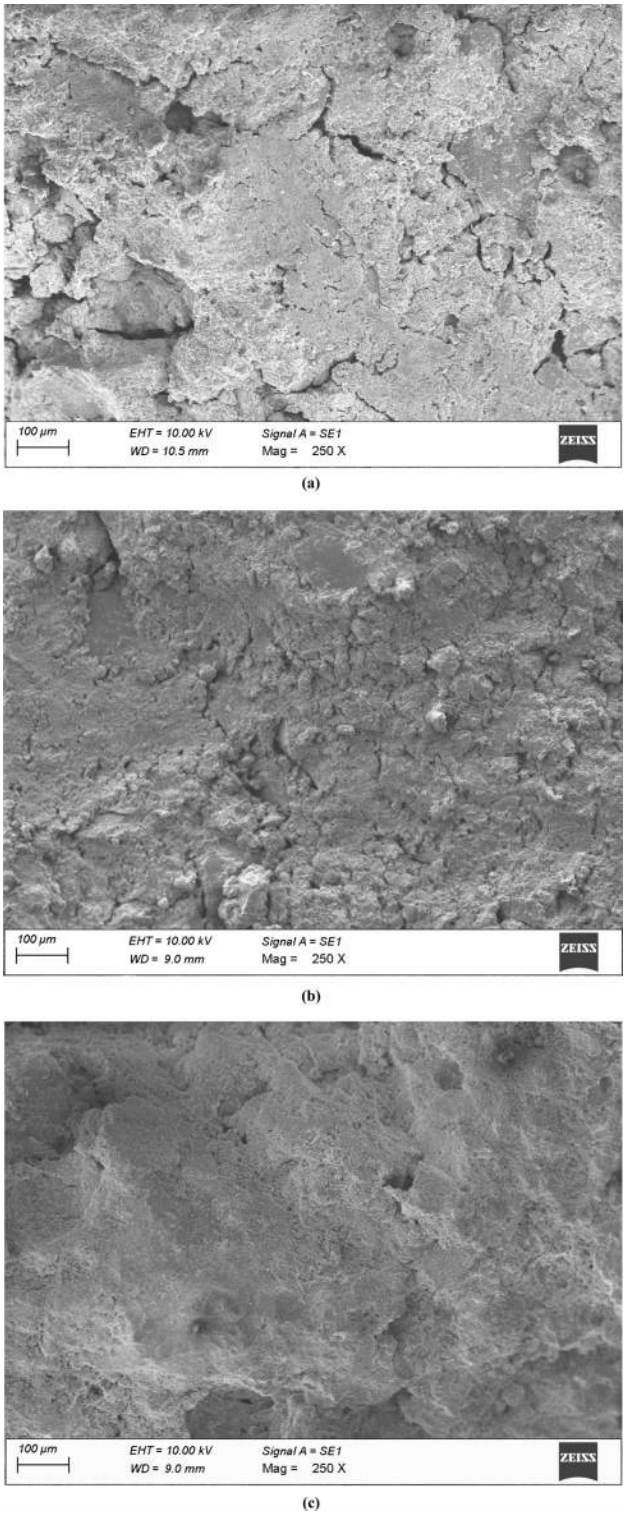


**Fig. 8.** Microstructure of various geopolymer mixes (a. F70M0, b. F50M50 and c. F30M50S20).

structural water resulting from the condensation of silanol and aluminol groups within the geopolymer gel. This process led to the creation of Si-O-T tetrahedral linkages, where T represents either Si or Al [36]. The mass loss during zone III fluctuated between 1% and 2%. Above 800 °C, no significant weight alteration was observed (zone IV), indicating the cessation of further thermal decomposition reactions. At the elevated temperature of 1200°C, the prepared geopolymers showcased mass retention ranging from 92.5% to 97.5%, underscoring their commendable thermal durability [37].

### Microstructural analysis

A scanning electron microscope (SEM) was used to examine microstructures. To better understand morphological properties, a comparison study was done on geopolymer concrete specimens F70M30, F50M50, and F30M50S20. Figures 8a, 8b and 8c depict visual representations of these specimens, respectively.

In the case of the F70M30 mixture, a notable observation was the presence of a substantial crack width and larger pore dimensions within the interfacial transition zone (ITZ), which contrasted sharply with the F50M50 mixture which showed a nominal crack width. These distinct characteristics in the microstructure aligned well with the discernibly weaker mechanical properties as elaborated upon in Table 4. This also indicated that the increase in MK content produced a compacted mix. Moreover, a comparative analysis of the microstructure of the F30M50S20 mixture, as depicted in Fig. 8c, revealed a smoother and less porous surface. The inclusion of SF led to well compacted structure, offering higher strength. This particular observation concurred with the findings of previously reported studies.

The outcomes from this microstructural analysis provided compelling evidence that the incorporation of supplementary materials, such as SF, contributed significantly to the enhancement of the bonding strength and overall uniformity between the geopolymer paste and the aggregates. These findings further corroborated the established and determined characteristics of strength in the material.

## Conclusion

The study introduced a novel approach to utilise ceramic waste aggregates (CWA) in eco-friendly geopolymer concrete, replacing conventional coarse aggregates (CCA). This involved incorporating class F fly ash (FFA), metakaolin (MK), silica fume (SF) and alkali activators to produce geopolymer concrete. The results can be summarised as follows.

- OPC-CWA mix (slump 122 mm) is more workable than OPC-CCA mix (slump 114 mm) due to CWA's lower water absorption. Geopolymer concrete is less workable than OPC due to high paste viscosity during geopolymerization. Replacing FFA with MK reduces slump due to particle differences, and silica fume decreases workability by absorbing water and filling gaps.
- OPC-CCA mix displayed the highest strengths due to the inherent properties of natural rock-based coarse crushed aggregate. Geopolymer mixes had lower early strengths but competitive strengths at 28 days. Increasing MK and SF content improved geopolymerization, denser microstructure, and enhanced compressive, splitting tensile and flexural strengths.
- Compressive strength of Concrete correlated with tensile and flexural strengths with high R2 values (0.9735 and 0.9824 respectively). OPC-CCA mix exhibited the highest UPV (3930 m/s), while geopolymers showed an UPV increase with MK content. MK-SF combinations improved UPV and internal quality. UPV also correlated well (R2 0.9153) with 28-day compressive strength for non-destructive strength estimation.
- XRD patterns reveal the mineral composition of geopolymer mixes, with quartz, CSH, and mullite phases. SF mixes exhibit higher geopolymeric compounds due to SF's reactivity, validating their mechanical properties. TGA profiles indicate mass loss stages at different temperatures due to water expulsion and structural changes. Geopolymers show notable thermal durability at 1200 °C.
- SEM analysis of geopolymer concrete specimens F70M30, F50M50, and F30M50S20 revealed microstructural differences. F70M30 exhibited wide cracks and larger pores in the ITZ, aligning with weaker mechanical properties. F50M50 showed a smaller crack width. F30M50S20 displayed a smoother, less porous surface due to SF inclusion, enhancing bonding and strength characteristics.

## References

1. G. Habert, S.A. Miller, V.M. John, J.L. Provis, A. Favier, A. Horvath, and K.L. Scrivener, Nat. Rev. Earth Environ. 1[11] (2020) 559-573.
2. Y. Wu, B. Lu, T. Bai, H. Wang, F. Du, Y. Zhang, L. Cai, C. Jiang, and W. Wang, Constr. Build. Mater. 224 (2019) 930-949.
3. N. Ranjbar, C. Kuenzel, J. Spangenberg, and M. Mehrali, Cem. Concr. Compos. 114 (2020) 103729.
4. H.L. Dinh, J.-H. Doh, J. Liu, L. Lu, H. Song, and D. Park, J. Build. Eng. 76 (2023) 107094.
5. M. Amran, A. Al-Fakih, S.H. Chu, R. Fediuk, S. Haruna, A. Azevedo, and N. Vatin, Case Stud. Constr. Mater. 15 (2021) e00661.
6. J. Li, Z. Wu, C. Shi, Q. Yuan, and Z. Zhang, Constr. Build. Mater. 255 (2020) 119296.
7. S. Parathi, P. Nagarajan, and S.A. Pallikkara, Clean Technol. Environ. Policy 23[6] (2021) 1701-1713.
8. B. Graybeal and J. Tanesi, J. Mater. Civ. Eng. 19[10] (2007) 848-854.
9. N.A. Soliman and A. Tagnit-Hamou, Constr. Build.

Mater. 145 (2017) 243-252.
10. Q. Chang, L. Liu, M.U. Farooqi, B. Thomas, and Y.O. Özkılıç, J. Mater. Res. Technol. 24 (2023) 6348-6368.
11. R.M. Senthamarai and P. Devadas Manoharan, Cem. Concr. Compos. 27[9] (2005) 910-913.
12. C. Medina, M.I. Sánchez de Rojas, and M. Frías, Cem. Concr. Compos. 34[1] (2012) 48-54.
13. H. Elçi, J. Cleaner Prod. 112 (2016) 742-752.
14. D.M. Kannan, S.H. Aboubakr, A.S. El-Dieb, and M.M. Reda Taha, Constr. Build. Mater. 144 (2017) 35-41.
15. A.S. El-Dieb, M.R. Taha, D. Kanaan, and S.T. Aly, Proc. Inst. Civ. Eng.: Constr. Mater. 171[3] (2018) 109-116.
16. M. Suzuki, M. Seddik Meddah, and R. Sato, Cem. Concr. Res. 39[5] (2009) 373-381.
17. S. Subaşı, H. Öztürk, and M. Emiroğlu, Constr. Build. Mater. 149 (2017) 567-574.
18. G.F. Huseien, A.R.M. Sam, K.W. Shah, J. Mirza, and M.M. Tahir, Constr. Build. Mater. 210 (2019) 78-92.
19. V. López, B. Llamas, A. Juan, J.M. Morán, and I. Guerra, Biosyst. Eng. 96[4] (2007) 559-564.
20. P. Torkittikul and A. Chaipanich, Cem. Concr. Compos. 32[6] (2010) 440-449.
21. Y. Kim and H. Kim, J. Ceram. Pro. Res. 23[2] (2022) 126-131.
22. Y. Kim and M. Kim, J. Ceram. Pro. Res. 20[5] (2019) 522-529.
23. M. Kim and Y. Kim, J. Ceram. Pro. Res. 22[2] (2021) 158-168.
24. S. Se-Gu, K. Young-Do, L. Woo-Keun, and K. Kyung-Nam, J. Ceram. Pro. Res. 14[5] (2013) 591-594.
25. S.K. Zakaria, N.I.N. Abd Rahman, S.Z. Salleh, N.M. Sharif, A.A. Seman, M.A.A. Taib, J.J. Mohamed, M. Yusoff, A.H. Yusoff, and M. Mohamad, J. Ceram. Process. Res. 22 (2021) 333-339.
26. Q. Tian, D. Sun, Z. Gu, and Z. Lv, J. Ceram. Pro. Res. 21[3] (2020) 358-364.
27. Y. Rho, J. Ceram. Pro. Res. 21 (2020) 74-80.
28. BIS, Bureau of Indian Standards, New Delhi, 2013.
29. S. Naenudon, A. Wongsa, J. Ekprasert, V. Sata, and P. Chindaprasirt, J. Build. Eng. 68 (2023) 106132.
30. P. Duan, C. Yan, and W. Zhou, Ceram. Int. 42[2] (2016) 3504-3517.
31. P. Nuaklong, V. Sata, and P. Chindaprasirt, Constr. Build. Mater. 161 (2018) 365-373.
32. T.A. Le, S.H. Le, T.N. Nguyen, and K.T. Nguyen, SN Appl. Sci. 11[7] (2021) 3032.
33. S. Samantasinghar and S.P. Singh, Int. J. Concr. Struct. Mater. 13[1] (2019) 1-12.
34. V.F.F. Barbosa and K.J.D. MacKenzie, Mater. Res. Bull. 38[2] (2003) 319-331.
35. M.F. Zawrah, S.E. Abo Sawan, R.M. Khattab, and A.A. Abdel-Shafi, Constr. Build. Mater. 246 (2020) 118486.
36. P. Duxson, G.C. Lukey, and J.S.J. van Deventer, J. Mater. Sci. 42[9] (2007) 3044-3054.
37. P.N. Lemougna, A. Adediran, J. Yliniemi, A. Ismailov, E. Levanen, P. Tanskanen, P. Kinnunen, J. Roning, and M. Illikainen, Cem. Concr. Compos. 114 (2020) 103792.